

Supporting information

CANDOCK: Chemical atomic network based hierarchical flexible docking algorithm using generalized statistical potentials

Jonathan Fine^{1,‡}, Janez Konc^{2,‡}, Ram Samudrala³, Gaurav Chopra^{1,4,5,6,7 *}

¹Department of Chemistry, Purdue University, 720 Clinic Drive, West Lafayette, IN 47906

²National Institute of Chemistry, Hajdrihova 19, SI-1000, Ljubljana, Slovenia ³Department of Biomedical Informatics, SUNY, Buffalo, NY, USA

⁴Purdue Institute for Drug Discovery

⁵Purdue Center for Cancer Research

⁶Purdue Institute for Inflammation, Immunology and Infectious Disease

⁷Purdue Institute for Integrative Neuroscience

[‡]These authors share equal contribution to this work.

*Corresponding Author

E-mail: gchopra@purdue.edu

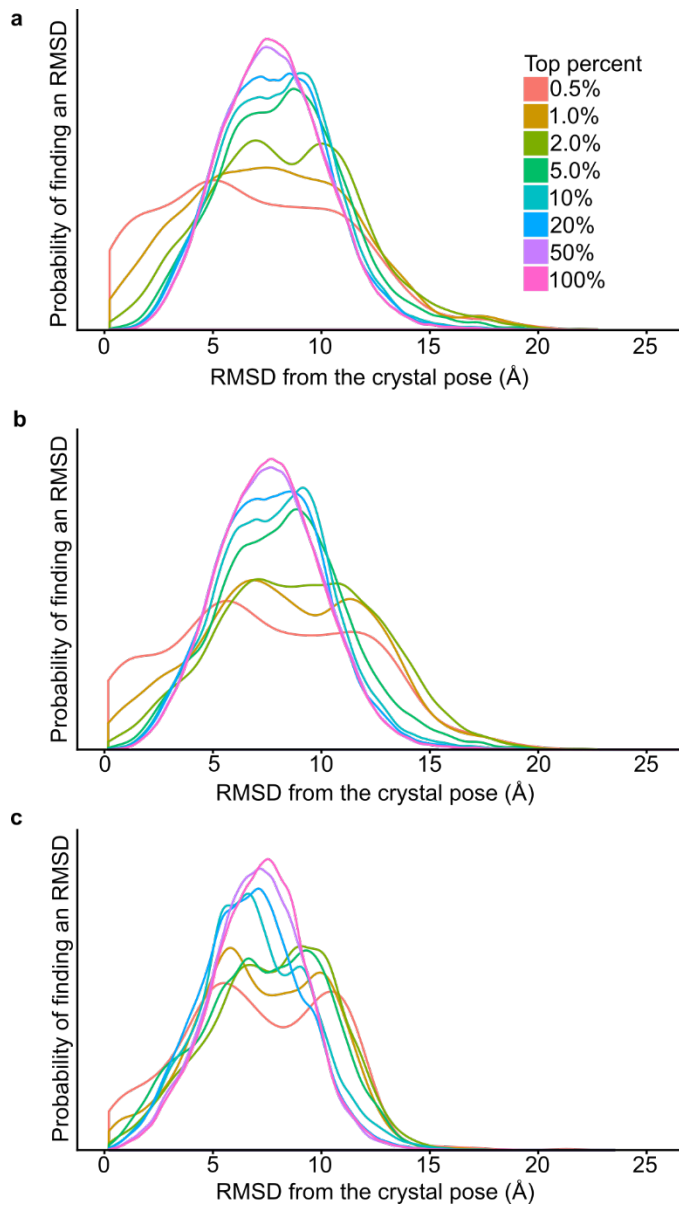


Figure S1: Distribution of RMSD values for all ligand poses generated by CANDOCK for the PDBbind Core set for **(a)** rigid-protein docking, **(b)** semi-flexible protein, and **(c)** fully-flexible protein docking.

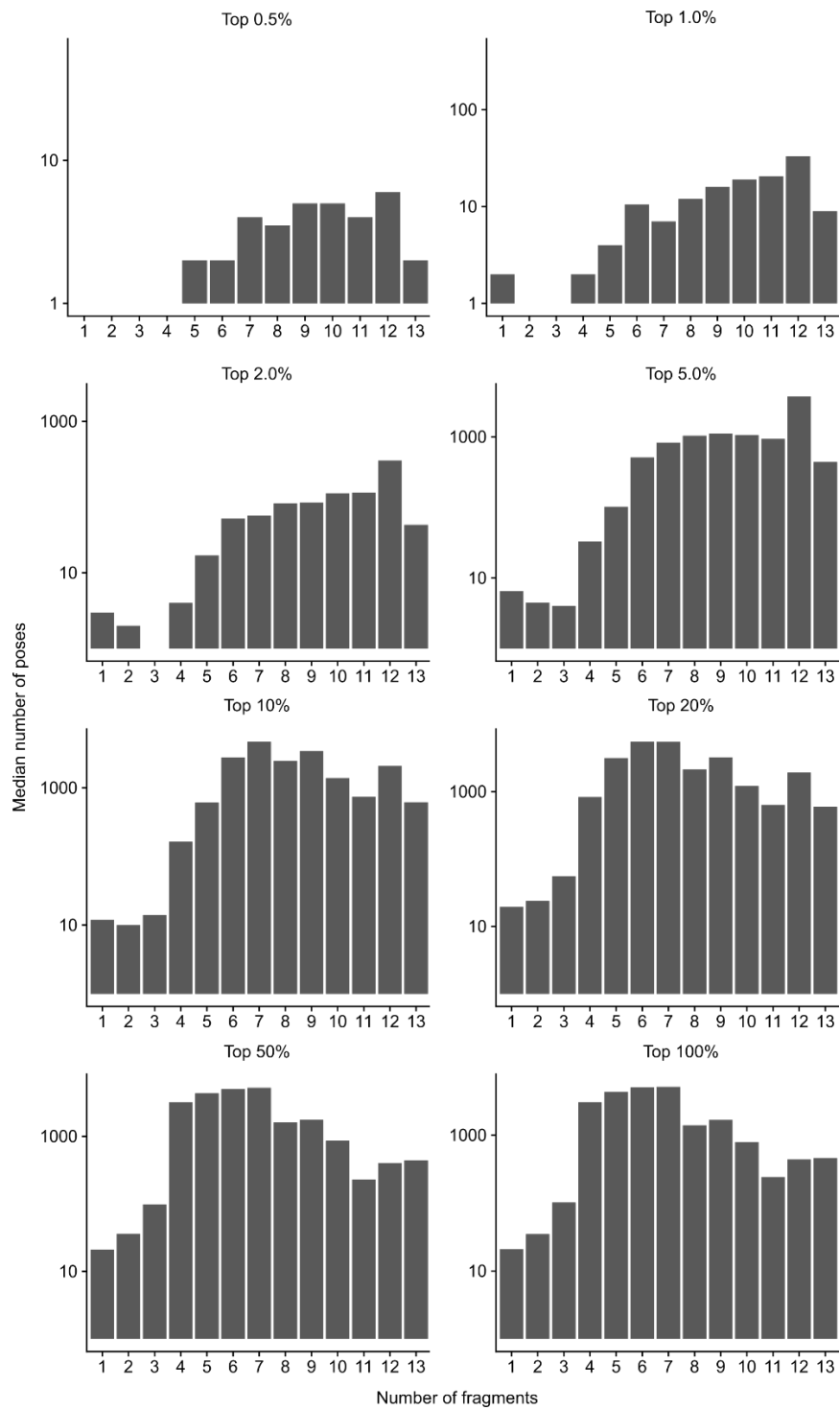


Figure S2: Median number of poses generated for ligands containing 1-13 fragments divided by the top percent parameter.

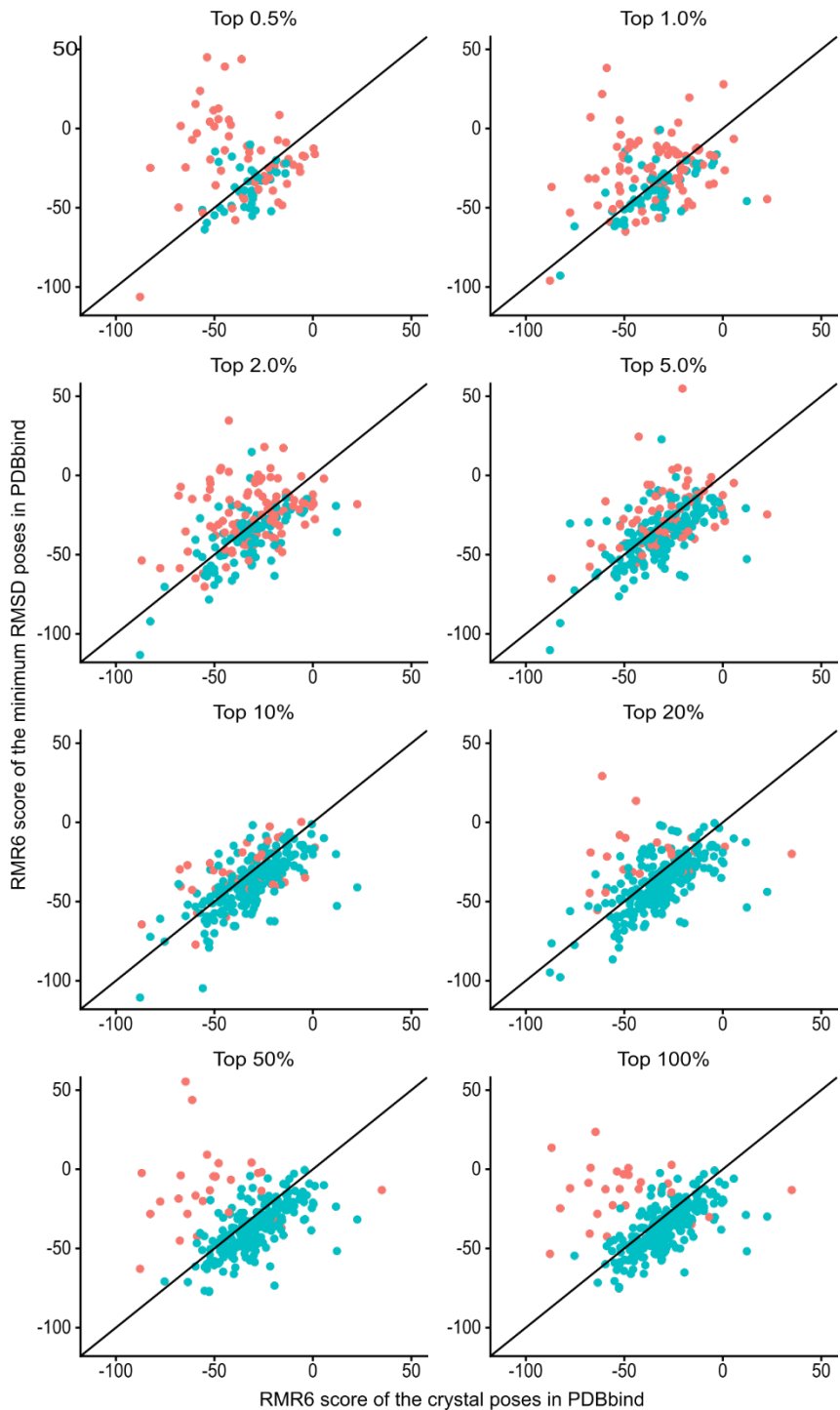


Figure S3: Correlations between the RMR6 scores of the crystal poses and the pose with the lowest RMSD are shown for all eight top percent values for complexes in the PDBbind Core set. Poses within 2.0 Å of the crystal pose are shown in blue (successful runs) while poses greater than 2.0 Å (failures) are shown in red. For top percent values greater than 20%, the complexes that failed cluster above the $y=x$ line. Therefore, in these cases, the CANDOCK algorithm did not sample the conformation space close to the binding pocket.

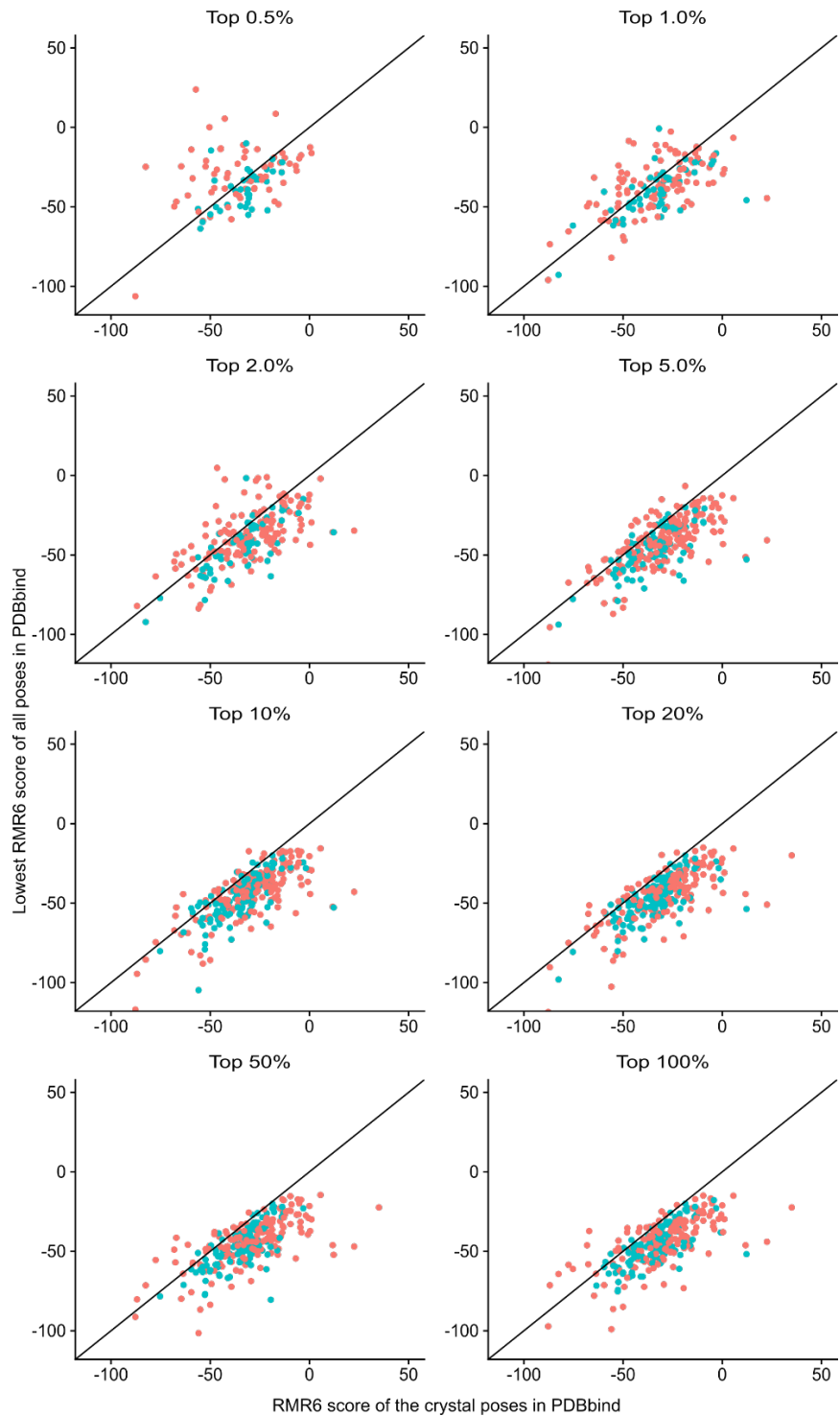


Figure S4: The lowest RMR6 score obtained for each cocrystal is plotted against the RMC15 score of the crystal pose. Poses within 2.0 Å of the crystal pose are shown in blue (successful runs) while poses greater than 2.0 Å are shown in red. The majority of points on this graph cluster below the $y=x$ line, indicating that the RMR6 scoring function incorrectly scores several poses more favorably than the crystal pose, regardless of if the pose is close to the crystal pose. Therefore, there are potential improvements to be made for this scoring function.

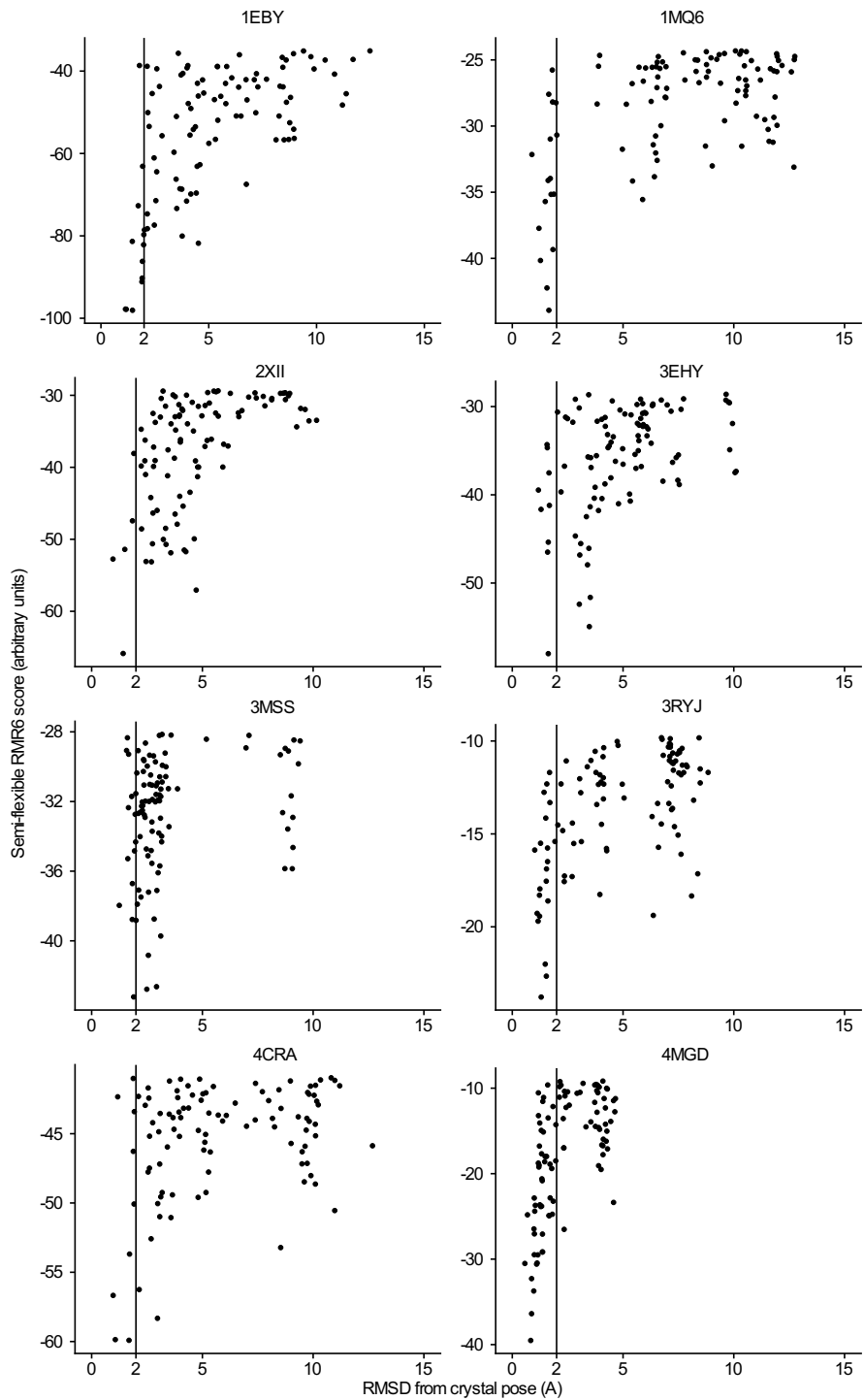


Figure S5: Plots of the RMR6 score of all poses produced by CANDOCK for selected proteins in the PDBbind Core Set versus the RMSD of the pose. In all plots, the RMSD ranges from 1 Å to 15 Å. The poses were obtained using the semi flexible method at a ‘Top Percent’ value equal to 20%. These of these plots show a tunnel like affect around as one approaches an RMSD of zero, showing the scoring functions ability to select the crystal pose in these cases.

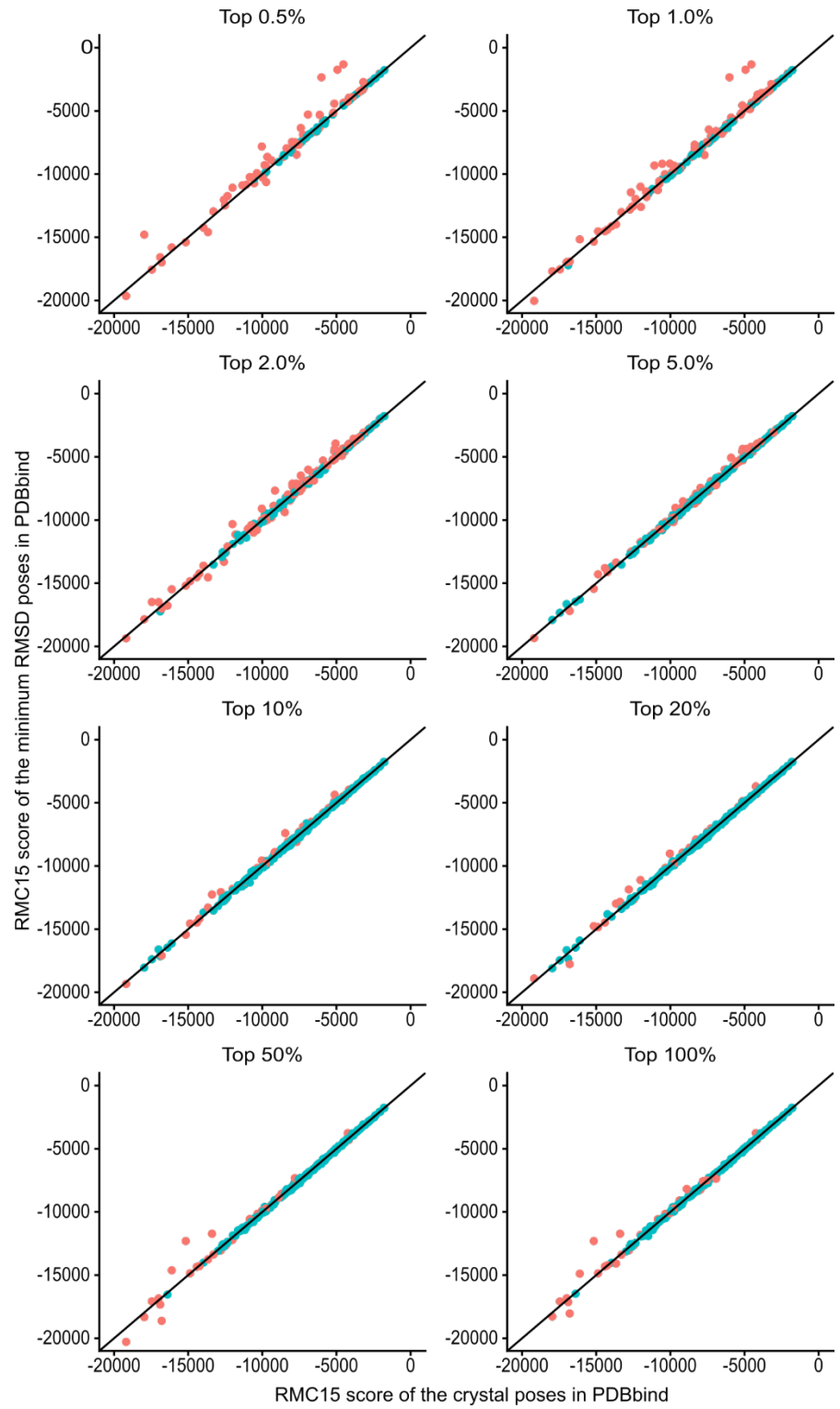


Figure S6: Correlations between the RMC15 scores of the crystal pose and the pose with the lowest RMSD are shown for all eight top percent values. Poses within 2.0 Å of the crystal pose are shown in blue (successful runs) while poses greater than 2.0 Å are shown in red.

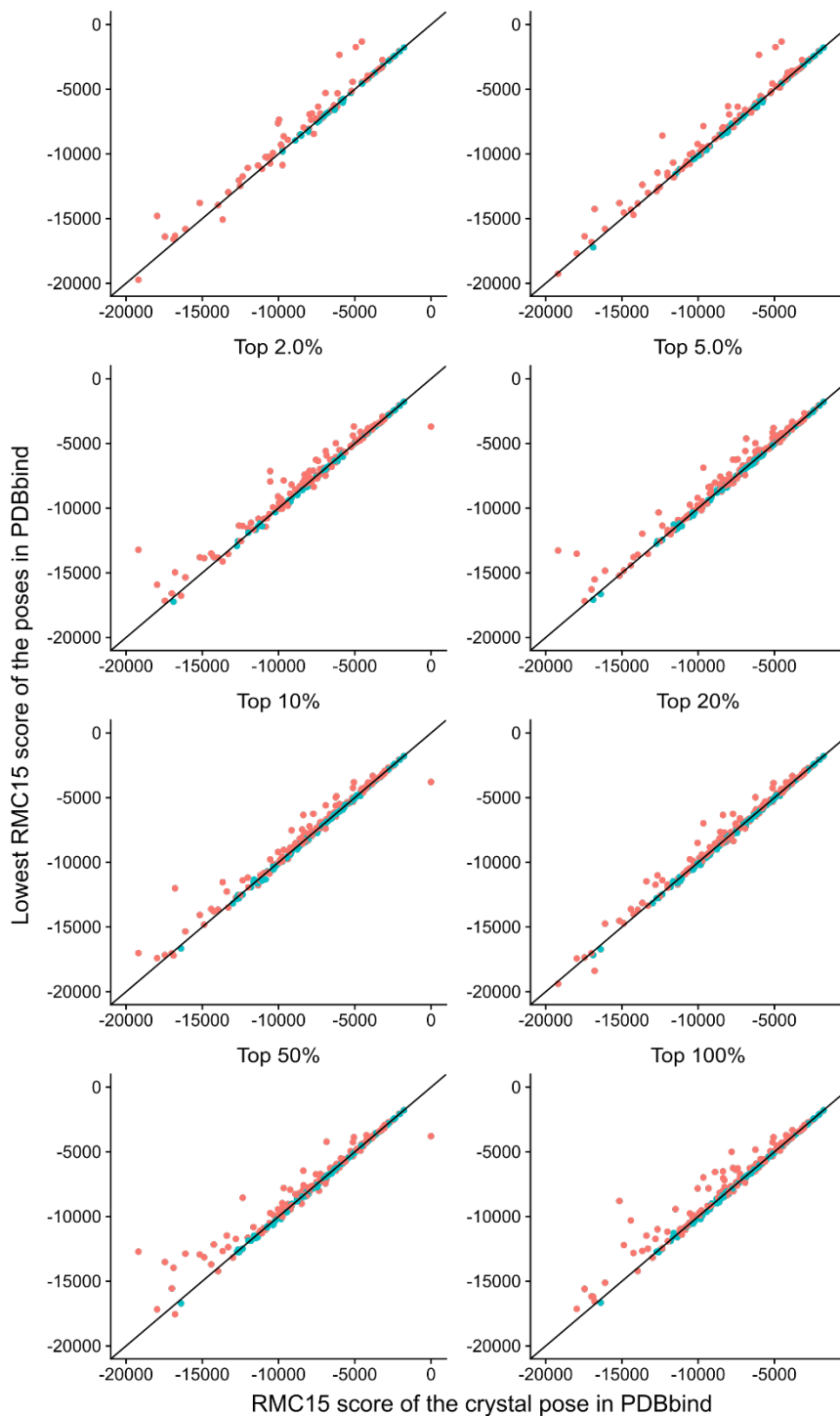


Figure S7: The RMC15 score for the pose selected by RMR6 obtained for each cocrystal is plotted against the RMC15 score of the crystal pose. Poses within 2.0 Å of the crystal pose are shown in blue (successful runs) while poses greater than 2.0 Å are shown in red. Here it is shown that the successful poses occur only on the $y=x$ line, while the unsuccessful poses cluster above this line. This indicates that further minimization with RMC15 may improve the RMR6 selection rate.

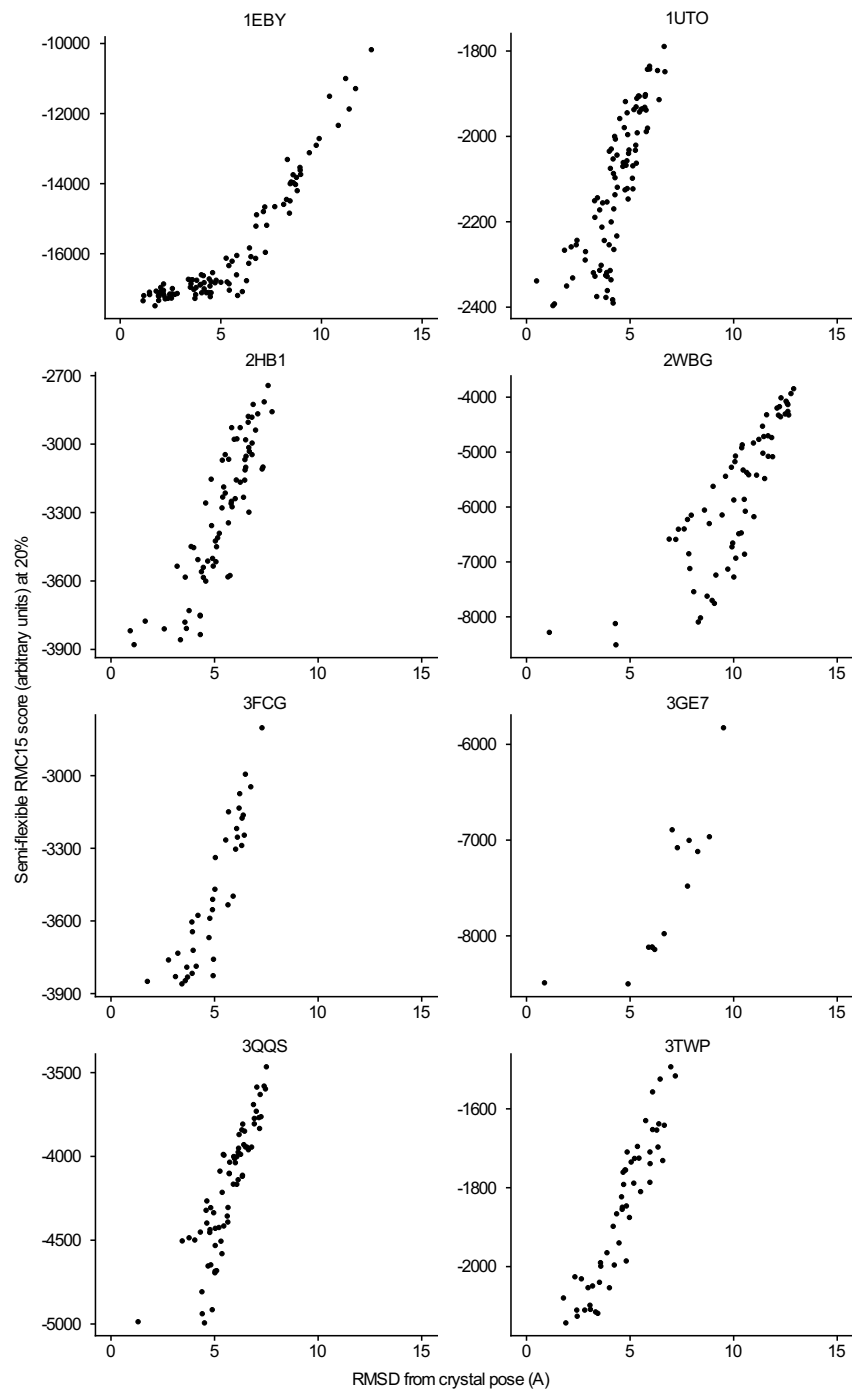
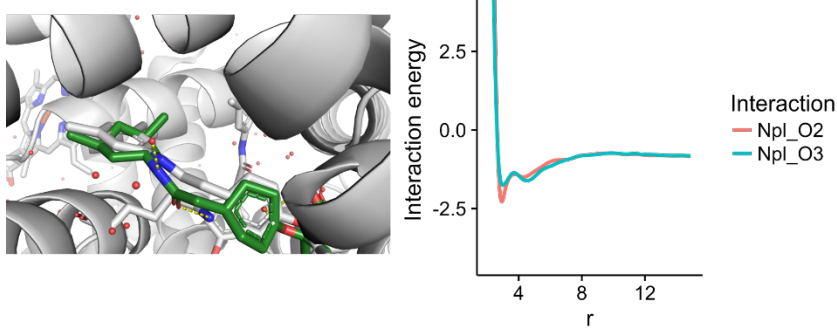
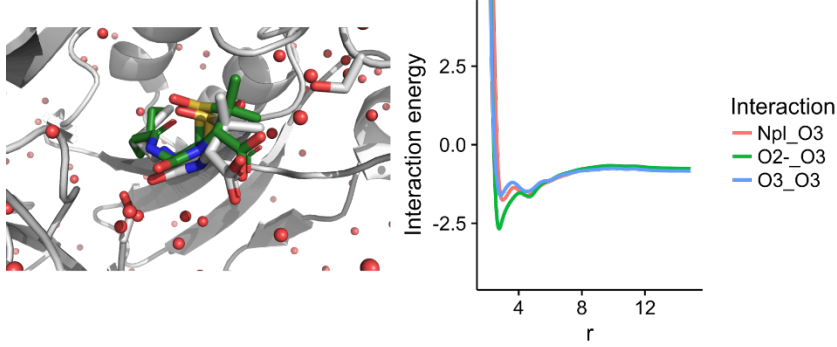


Figure S8: Plots of the RMC15 score of all poses produced by CANDOCK for selected proteins in the PDBbind Core Set versus the RMSD of the pose. In all plots, the RMSD ranges from 1 Å to 15 Å. The poses were obtained using the semi flexible method at a ‘Top Percent’ value equal to 20%. The trend seen for these proteins is as one decreases the RMC15 score, the RMSD of the predicted ligand also decreases. Therefore, the use of an objective function derived from the RMC15 scoring function to minimize the ligand in the binding pocket is justified.

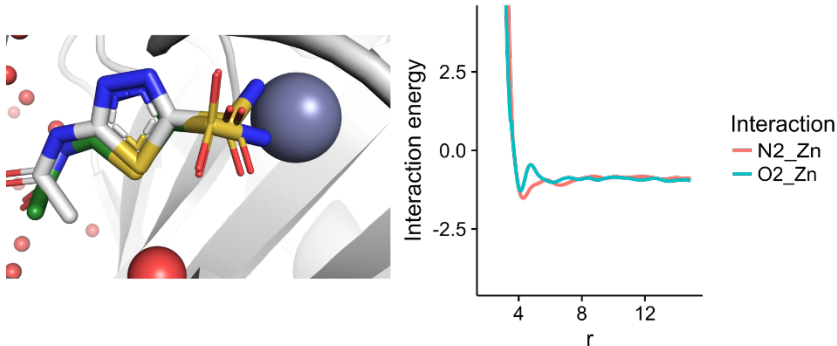
1G9V



1GM8



1DJ0



1MEH

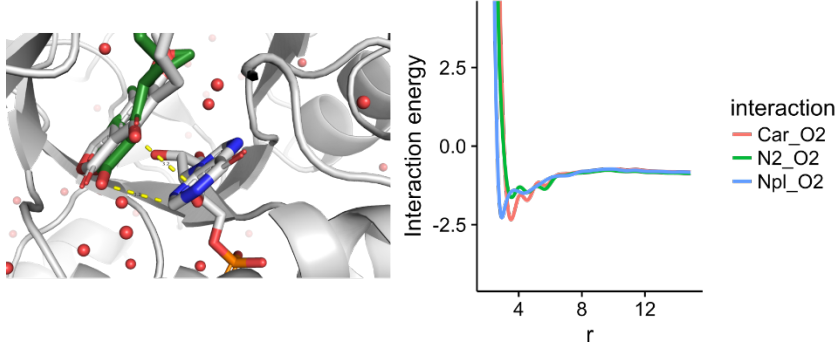


Figure S9: Examples where CANDOCK is able to produce a good docking pose where other methods are not able. The best CANDOCK pose is given on the lefthand side of the figure and important interactions between the ligand protein are given on the right.

	Rigid protein		Semi-flexible protein		Fully-flexible protein	
	Average	Median	Average	Median	Average	Median
rnr4	0.095	0.049	0.095	0.049	0.140	0.080
rnr5	0.145	0.102	0.145	0.102	0.180	0.113
rnr6	0.176	0.115	0.176	0.115	0.189	0.130
rnr7	0.178	0.112	0.178	0.112	0.207	0.139
rnr8	0.190	0.112	0.190	0.112	0.212	0.165
rnr9	0.189	0.123	0.189	0.123	0.214	0.182
rnr10	0.203	0.141	0.203	0.141	0.236	0.212
rnr11	0.216	0.149	0.216	0.149	0.253	0.230
rnr12	0.225	0.165	0.225	0.165	0.262	0.246
rnr13	0.222	0.181	0.222	0.181	0.261	0.256
rnr14	0.210	0.169	0.210	0.169	0.249	0.236
rnr15	0.183	0.121	0.183	0.121	0.217	0.196
rmc4	0.307	0.279	0.307	0.279	0.361	0.360
rmc5	0.413	0.416	0.413	0.416	0.424	0.426
rmc6	0.459	0.473	0.459	0.473	0.462	0.471
rmc7	0.476	0.501	0.476	0.501	0.495	0.498
rmc8	0.498	0.519	0.498	0.519	0.518	0.528
rmc9	0.523	0.542	0.523	0.542	0.538	0.555
rmc10	0.537	0.560	0.537	0.560	0.550	0.559
rmc11	0.539	0.562	0.539	0.562	0.554	0.565
rmc12	0.546	0.571	0.546	0.571	0.561	0.579
rmc13	0.546	0.576	0.546	0.576	0.562	0.584
rmc14	0.556	0.587	0.556	0.587	0.560	0.587
rmc15	0.559	0.581	0.559	0.581	0.559	0.587
fmr4	0.081	0.027	0.081	0.027	0.121	0.071
fmr5	0.107	0.063	0.107	0.063	0.144	0.094
fmr6	0.125	0.064	0.125	0.064	0.155	0.106
fmr7	0.132	0.069	0.132	0.069	0.166	0.108
fmr8	0.152	0.079	0.152	0.079	0.177	0.102
fmr9	0.149	0.078	0.149	0.078	0.183	0.112
fmr10	0.149	0.070	0.149	0.070	0.183	0.114
fmr11	0.146	0.075	0.146	0.075	0.179	0.119
fmr12	0.135	0.062	0.135	0.062	0.164	0.114
fmr13	0.116	0.048	0.116	0.048	0.140	0.084
fmr14	0.093	0.023	0.093	0.023	0.110	0.053
fmr15	0.062	-0.014	0.062	-0.014	0.071	0.009
fmc4	0.307	0.270	0.307	0.270	0.360	0.353
fmc5	0.424	0.427	0.424	0.427	0.429	0.430
fmc6	0.468	0.480	0.468	0.480	0.468	0.480

fmc7	0.486	0.510	0.486	0.510	0.501	0.509
fmc8	0.505	0.527	0.505	0.527	0.523	0.530
fmc9	0.535	0.549	0.535	0.549	0.541	0.563
fmc10	0.539	0.560	0.539	0.560	0.552	0.563
fmc11	0.539	0.562	0.539	0.562	0.554	0.570
fmc12	0.545	0.569	0.545	0.569	0.561	0.581
fmc13	0.546	0.580	0.546	0.580	0.562	0.583
fmc14	0.556	0.587	0.556	0.587	0.558	0.586
fmc15	0.559	0.582	0.559	0.582	0.557	0.583
rcr4	0.050	-0.015	0.050	-0.015	0.115	0.053
rcr5	0.053	-0.015	0.053	-0.015	0.103	0.043
rcr6	0.056	-0.016	0.056	-0.016	0.096	0.036
rcr7	0.047	-0.018	0.047	-0.018	0.084	0.025
rcr8	0.057	-0.010	0.057	-0.010	0.090	0.022
rcr9	0.053	-0.013	0.053	-0.013	0.085	0.033
rcr10	0.039	-0.025	0.039	-0.025	0.066	0.007
rcr11	0.031	-0.035	0.031	-0.035	0.055	0.010
rcr12	0.031	-0.034	0.031	-0.034	0.054	0.007
rcr13	0.038	-0.031	0.038	-0.031	0.064	0.024
rcr14	0.057	-0.017	0.057	-0.017	0.089	0.037
rcr15	0.081	-0.006	0.081	-0.006	0.120	0.069
rcc4	0.067	0.001	0.067	0.001	0.119	0.047
rcc5	0.075	0.007	0.075	0.007	0.112	0.047
rcc6	0.073	0.013	0.073	0.013	0.099	0.040
rcc7	0.056	-0.005	0.056	-0.005	0.078	0.021
rcc8	0.051	-0.012	0.051	-0.012	0.067	0.000
rcc9	0.036	-0.028	0.036	-0.028	0.048	-0.010
rcc10	0.020	-0.053	0.020	-0.053	0.024	-0.028
rcc11	0.011	-0.073	0.011	-0.073	0.013	-0.043
rcc12	0.013	-0.072	0.013	-0.072	0.013	-0.043
rcc13	0.021	-0.061	0.021	-0.061	0.025	-0.030
rcc14	0.040	-0.044	0.040	-0.044	0.049	-0.009
rcc15	0.065	-0.010	0.065	-0.010	0.081	0.020
fcr4	0.050	-0.015	0.050	-0.015	0.115	0.062
fcr5	0.062	-0.002	0.062	-0.002	0.113	0.060
fcr6	0.071	-0.001	0.071	-0.001	0.117	0.056
fcr7	0.074	0.003	0.074	0.003	0.122	0.057
fcr8	0.084	0.014	0.084	0.014	0.130	0.070
fcr9	0.086	0.007	0.086	0.007	0.132	0.073
fcr10	0.091	0.011	0.091	0.011	0.138	0.072
fcr11	0.102	0.033	0.102	0.033	0.154	0.106

fcr12	0.116	0.047	0.116	0.047	0.171	0.115
fcr13	0.133	0.063	0.133	0.063	0.193	0.144
fcr14	0.157	0.091	0.157	0.091	0.221	0.181
fcr15	0.177	0.116	0.177	0.116	0.244	0.209
fcc4	0.063	-0.006	0.063	-0.006	0.112	0.054
fcc5	0.075	0.002	0.075	0.002	0.111	0.055
fcc6	0.084	0.019	0.084	0.019	0.116	0.057
fcc7	0.088	0.026	0.088	0.026	0.122	0.059
fcc8	0.098	0.021	0.098	0.021	0.131	0.064
fcc9	0.101	0.029	0.101	0.029	0.134	0.070
fcc10	0.105	0.036	0.105	0.036	0.141	0.076
fcc11	0.117	0.053	0.117	0.053	0.157	0.100
fcc12	0.132	0.071	0.132	0.071	0.175	0.121
fcc13	0.146	0.086	0.146	0.086	0.193	0.138
fcc14	0.163	0.107	0.163	0.107	0.215	0.165
fcc15	0.179	0.126	0.179	0.126	0.233	0.192

Table S1: Correlations between score and small molecule RMSD calculated and summarized over the entire PDBbind Core benchmarking set.

Selector:	RMSD		RMR6		RMC15	
Ranker	RMR6	RMC15	RMR6	RMC15	RMR6	RMC15
3-DEHYDROQUINATE DEHYDRATASE	-0.716	-0.876	-0.852	-0.875	0.591	-0.874
ACETYLCHOLINE RECEPTOR	0.335	0.339	0.476	0.350	0.772	0.326
ACETYLCHOLINE-BINDING PROTEIN	0.482	-0.193	-0.004	-0.195	0.554	-0.212
ACHE	-0.269	-0.664	-0.474	-0.688	-0.300	-0.652
ALPHA-L-FUCOSIDASE	-0.692	-0.372	-0.606	-0.307	-0.666	-0.304
ALPHA-MANNOSIDASE II	-0.271	-0.581	0.575	-0.580	0.855	-0.599
ANDROGEN RECEPTOR	-0.919	0.734	-0.738	0.730	-0.776	0.736
TrpD	0.652	-0.905	-0.328	-0.832	0.539	-0.920
BETA-GLUCOSIDASE A	0.751	0.140	-0.337	0.119	-0.953	0.147
BETA-LACTAMASE	-0.495	-0.894	-0.681	-0.908	0.835	-0.886
BETA-LACTOGLOBULIN	-0.981	-0.991	-0.978	-0.997	-0.959	-0.993
BETA-SECRETASE 1	0.695	-0.116	-0.210	-0.370	0.673	-0.121
BROMODOMAIN-CONTAINING PROTEIN 4	-0.644	-0.981	-0.579	-0.988	0.393	-0.955
CAMP-DEPENDENT PROTEIN KINASE	0.696	-0.905	-0.619	-0.996	0.785	-0.864
CARBONIC ANHYDRASE 2	-0.694	-0.883	0.770	-0.770	0.976	-0.856
CATECHOL O-METHYLTRANSFERASE	-0.858	-0.870	-0.749	-0.839	-0.687	-0.781
CELL DIVISION PROTEIN KINASE 2	-0.800	-0.899	0.713	-0.918	0.969	-0.879
CELLULAR TUMOR ANTIGEN P53	-0.739	-0.719	0.796	-0.719	0.925	-0.648
CGMP 3',5'-CYCLIC PHOSPHODIESTERASE	-0.649	0.052	-0.138	0.103	-0.711	0.074
CHITINASE A	-0.915	-0.725	-0.833	-0.725	-0.704	-0.682
COAGULATION FACTOR XA	-0.963	-0.753	-0.992	-0.671	0.560	-0.596
FACTOR XI	-0.805	-0.916	-0.864	-0.885	0.989	-0.887
DEHYDROSQUALENE SYNTHASE	-0.353	-0.439	-0.727	-0.468	0.173	-0.432
ENDOTHIAPEPSIN	-0.975	-0.993	-0.903	-0.992	0.971	-0.989
ESTROGEN RECEPTOR	-0.843	0.764	0.501	0.764	-0.293	0.761
GLUTAMATE RECEPTOR 2	-0.814	-0.457	-0.741	-0.458	-0.854	-0.454
GLUTAMATE RECEPTOR, IONOTROPIC KAINATE 1	-0.977	-0.646	-0.702	-0.632	0.872	-0.577
GLYCOGEN PHOSPHORYLASE	0.716	0.383	-0.186	0.407	-0.833	0.341
HEAT SHOCK PROTEIN HSP82	-0.418	0.112	-0.574	0.105	-0.771	0.166
HEAT SHOCK PROTEIN HSP90-ALPHA	-0.728	-0.879	-0.832	-0.882	0.778	-0.873
HIV-1 INTEGRASE	-0.843	-0.954	-0.954	-0.960	0.935	-0.952
HIV-1 PROTEASE	-0.916	-0.573	-0.907	-0.468	-0.926	-0.541
(MMP-1)	-0.680	-0.815	-0.801	-0.808	0.966	-0.796
MITOGEN-ACTIVATED PROTEIN KINASE 14	-0.680	-0.902	-0.691	-0.903	0.916	-0.900
MTA/SAH NUCLEOSIDASE	0.601	0.203	0.601	0.203	0.657	0.206
O-GLCNACASE BT_4395	-0.974	-0.128	-0.471	-0.129	-0.392	-0.074
PANTOTHENATE SYNTHETASE	-0.873	-0.960	-0.764	-0.961	0.835	-0.962
PPARG	-0.974	-0.992	-0.971	-0.989	0.902	-0.983
PROTEIN-TYROSINE PHOSPHATASE 1B	0.304	-0.947	-0.080	-0.805	0.759	-0.874

QUEUINE TRNA-RIBOSYLTRANSFERASE	-0.875	-0.697	-0.875	-0.697	-0.676	-0.703
RIBONUCLEASE A	-0.701	-0.842	-0.908	-0.849	0.708	-0.836
RNA-DIRECTED RNA POLYMERASE	-0.794	-0.831	-0.740	-0.828	0.981	-0.856
SERINE/THREONINE-PROTEIN KINASE 6	-0.093	-0.706	0.091	-0.885	-0.603	-0.619
CHK1	0.509	0.545	-0.204	0.637	0.963	0.386
PIM-1	0.656	0.447	0.423	0.436	-0.568	0.424
TANKYRASE-2	-0.918	-0.854	-0.970	-0.881	0.491	-0.825
THERMOLYSIN	-0.610	0.178	-0.546	-0.272	-0.700	0.149
THROMBIN	-0.798	0.154	0.473	0.188	0.562	0.155
TRANSCRIPTION ELONGATION FACTOR B POLYPEPTIDE 2	0.789	-0.772	0.784	-0.756	0.908	-0.770
TRANSPORTER	-0.376	0.497	-0.284	0.509	-0.352	0.510
TRYPSIN BETA	-0.905	-0.805	-0.927	-0.804	0.653	-0.769
TYROSINE-PROTEIN KINASE ABL1	0.929	-0.119	0.187	0.093	0.847	-0.221
TYROSINE-PROTEIN KINASE ITK/TSK	0.879	0.749	0.183	0.747	-0.786	0.755
TYROSINE-PROTEIN KINASE JAK1	-0.552	-0.093	-0.292	-0.154	0.234	-0.079
TYROSINE-PROTEIN KINASE JAK2	-0.653	-0.883	-0.718	-0.876	0.759	-0.931
UROKINASE-TYPE PLASMINOGEN ACTIVATOR	-0.909	-0.927	-0.908	-0.922	0.882	-0.924

Table S2: Pearson correlations for all ligands in the PDBbind Core set using various scoring functions to select the representative pose for the protein-ligand complex and rank the activity of the ligand versus other ligands for the same protein. Highlighted values are plotted in **Figure S7**.

Selector	RMSD		RMR6		RMC15	
Ranker	RMR6	RMC15	RMR6	RMC15	RMR6	RMC15
3-DEHYDROQUINATE DEHYDRATASE	-0.400	-0.600	-1.000	-0.600	0.700	-0.600
ACETYLCHOLINE RECEPTOR	0.400	0.100	0.600	0.100	0.600	0.100
ACETYLCHOLINE-BINDING PROTEIN	0.500	-0.300	-0.600	-0.300	0.700	-0.300
ACHE	-0.500	-0.700	-0.400	-0.700	-0.300	-0.700
ALPHA-L-FUCOSIDASE	-0.700	0.400	-0.700	0.400	-0.700	0.400
ALPHA-MANNOSIDASE II	-0.300	-0.300	0.300	-0.300	0.700	-0.300
ANDROGEN RECEPTOR	-0.700	0.900	-0.600	0.900	-1.000	0.900
TrpD	0.500	-1.000	-0.500	-0.900	0.300	-1.000
BETA-GLUCOSIDASE A	0.700	0.300	-0.400	0.300	-1.000	0.300
BETA-LACTAMASE	-0.455	-0.782	-0.745	-0.879	0.758	-0.782
BETA-LACTOGLOBULIN	-1.000	-1.000	-1.000	-1.000	-1.000	-1.000
BETA-SECRETASE 1	0.500	0.000	-0.300	-0.400	0.700	0.000
BROMODOMAIN-CONTAINING PROTEIN 4	-0.700	-0.900	-0.600	-1.000	0.200	-0.900
CAMP-DEPENDENT PROTEIN KINASE	0.700	-1.000	-0.400	-1.000	0.600	-1.000
CARBONIC ANHYDRASE 2	-0.600	-0.800	0.700	-0.800	0.900	-0.800
CATECHOL O-METHYLTRANSFERASE	-0.800	-0.900	-0.700	-0.900	-0.900	-0.900
CELL DIVISION PROTEIN KINASE 2	-0.600	-0.700	0.500	-0.700	0.900	-0.700
CELLULAR TUMOR ANTIGEN P53	-0.900	-0.700	0.900	-0.700	0.900	-0.400
CGMP 3',5'-CYCLIC PHOSPHODIESTERASE	-0.700	0.000	-0.300	0.000	-0.700	0.000
CHITINASE A	-0.900	-0.700	-0.900	-0.700	-0.800	-0.700
FACTOR XA	-0.900	-0.900	-1.000	-0.900	0.700	-0.900
FACTOR XI	-0.700	-0.600	-0.700	-0.300	0.900	-0.300
DEHYDROSQUALENE SYNTHASE	-0.600	-0.100	-0.800	-0.200	0.500	-0.600
ENDOTHIAPEPSIN	-1.000	-1.000	-0.900	-0.900	1.000	-0.900
ESTROGEN RECEPTOR	-0.800	0.300	0.300	0.300	-0.600	0.300
GLUTAMATE RECEPTOR 2	-0.700	-0.700	-0.700	-0.700	-0.900	-0.700
GLUTAMATE RECEPTOR, IONOTROPIC KAINATE 1	-1.000	-0.700	-0.700	-0.700	0.900	-0.700
GLYCOGEN PHOSPHORYLASE	0.900	0.300	0.200	0.300	-0.800	0.300
HEAT SHOCK PROTEIN HSP82	-0.500	0.400	-0.600	0.400	-0.800	0.400
HEAT SHOCK PROTEIN HSP90-ALPHA	-0.600	-0.800	-0.700	-0.800	0.900	-0.800
HIV-1 INTEGRASE	-0.900	-1.000	-0.900	-1.000	0.700	-1.000
HIV-1 PROTEASE	-0.900	-0.700	-0.900	-0.800	-1.000	-0.600
MMP-12	-0.900	-0.900	-0.900	-0.900	0.900	-0.900
MITOGEN-ACTIVATED PROTEIN KINASE 14	-0.700	-0.900	-0.700	-1.000	0.900	-0.900
MTA/SAH NUCLEOSIDASE	0.700	-0.100	0.700	-0.100	0.600	-0.100
O-GLCNACASE BT_4395	-0.900	-0.600	-0.500	-0.600	-0.600	-0.600
PANTOTHENATE SYNTHETASE	-0.900	-1.000	-0.900	-1.000	0.800	-1.000
PPARG	-0.700	-1.000	-1.000	-1.000	1.000	-1.000

PROTEIN-TYROSINE PHOSPHATASE 1B	0.400	-1.000	-0.300	-0.700	0.700	-0.900
QUEUINE TRNA-RIBOSYLTRANSFERASE	-0.700	-0.600	-0.700	-0.600	-0.600	-0.600
RIBONUCLEASE A	-0.700	-0.700	-0.900	-0.700	0.400	-0.700
RNA-DIRECTED RNA POLYMERASE	-0.600	-1.000	-0.900	-1.000	1.000	-1.000
SERINE/THREONINE-PROTEIN KINASE 6	-0.500	-0.900	-0.500	-0.900	-0.600	-0.700
CHK1	0.600	0.600	-0.400	0.600	1.000	0.600
PIM-1	0.300	0.300	0.200	0.300	-0.300	0.300
TANKYRASE-2	-1.000	-0.800	-0.900	-0.900	0.500	-0.800
THERMOLYSIN	-0.600	0.000	-0.600	-0.400	-0.400	0.000
THROMBIN	-0.800	0.400	0.300	0.400	0.500	0.200
TCEB2	0.700	-0.700	0.800	-0.700	0.800	-0.700
TRANSPORTER	-0.500	0.700	-0.300	0.700	-0.600	0.700
TRYPSIN BETA	-0.900	-0.800	-0.900	-0.800	0.600	-0.800
TYROSINE-PROTEIN KINASE ABL1	1.000	-0.300	-0.400	-0.300	0.900	-0.300
TYROSINE-PROTEIN KINASE ITK/TSK	0.900	0.700	-0.100	0.700	-0.400	0.500
TYROSINE-PROTEIN KINASE JAK1	-0.600	-0.300	-0.600	-0.300	0.500	-0.300
TYROSINE-PROTEIN KINASE JAK2	-0.700	-0.900	-0.900	-0.900	0.700	-0.900
UROKINASE-TYPE PLASMINOGEN ACTIVATOR	-0.900	-0.900	-0.900	-0.900	1.000	-0.900

Table S3: Spearman correlations for all ligands in the PDBbind Core set using various scoring functions to select the representative pose for the protein-ligand complex and rank the activity of the ligand versus other ligands for the same protein. Highlighted values are plotted in **Figure S7**.

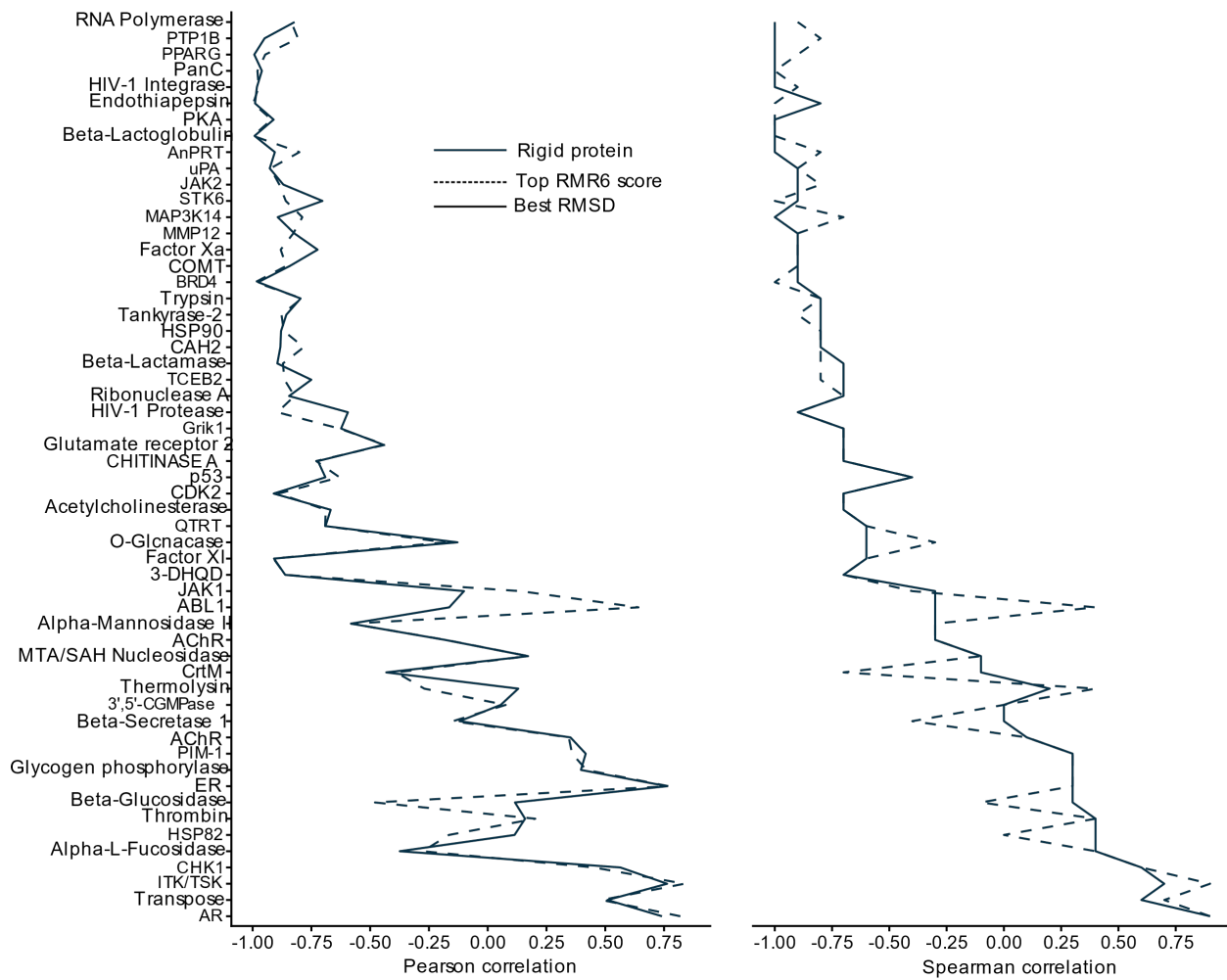


Figure S10: Rigid protein docking correlations between the RMC15 score and the measured pKd/pKi of the compounds in the PDBbind for each protein target. The representative docked ligand pose for ranking was selected with either the lowest RMSD or the best RMR6 score criterion.

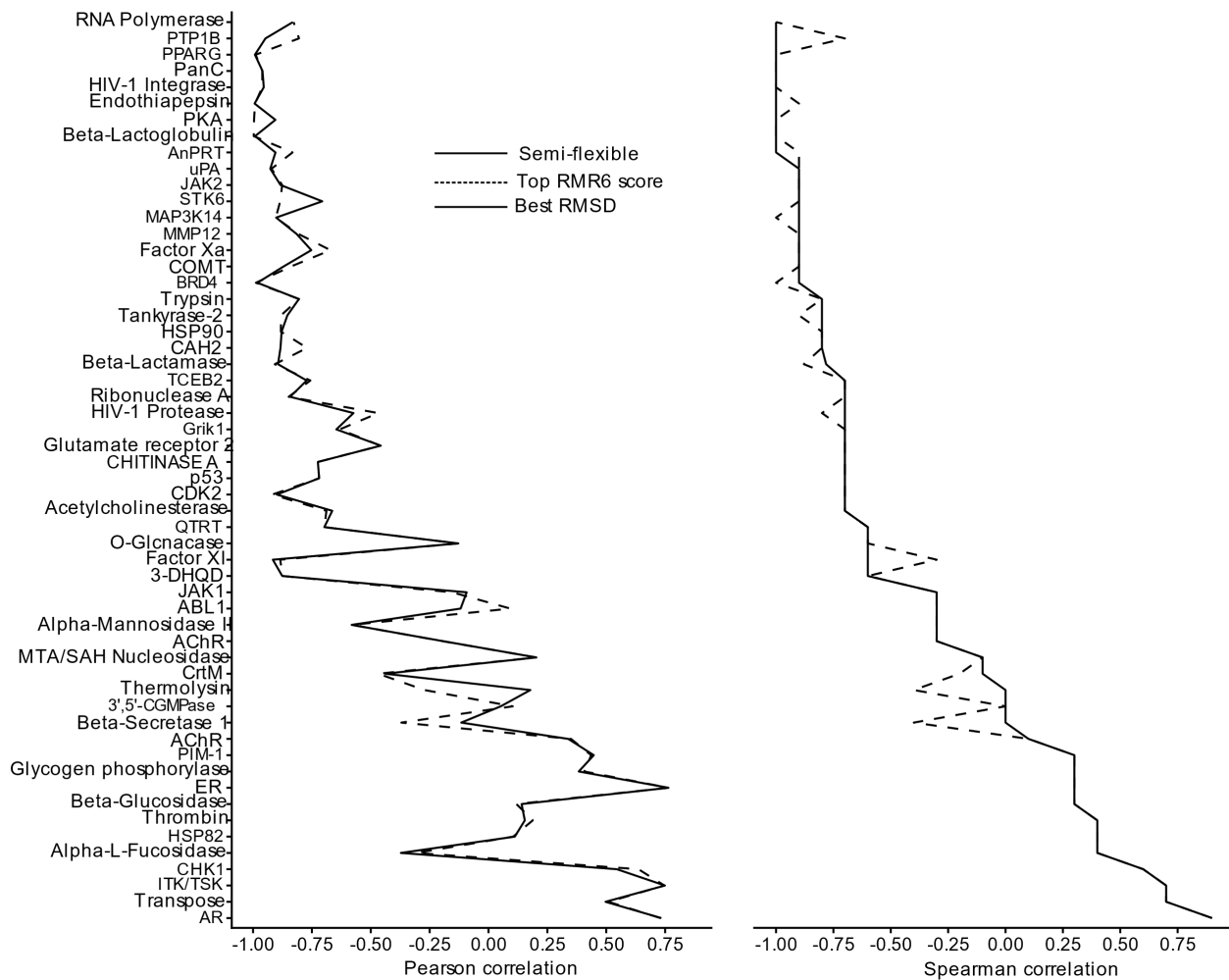


Figure S11: Semi-flexible protein docking correlations between the RMC15 score and the measured pKd/pKi of the compounds in the PDBbind for each protein target. The representative docked ligand pose for ranking was selected with either the lowest RMSD or the best RMR6 score criterion.

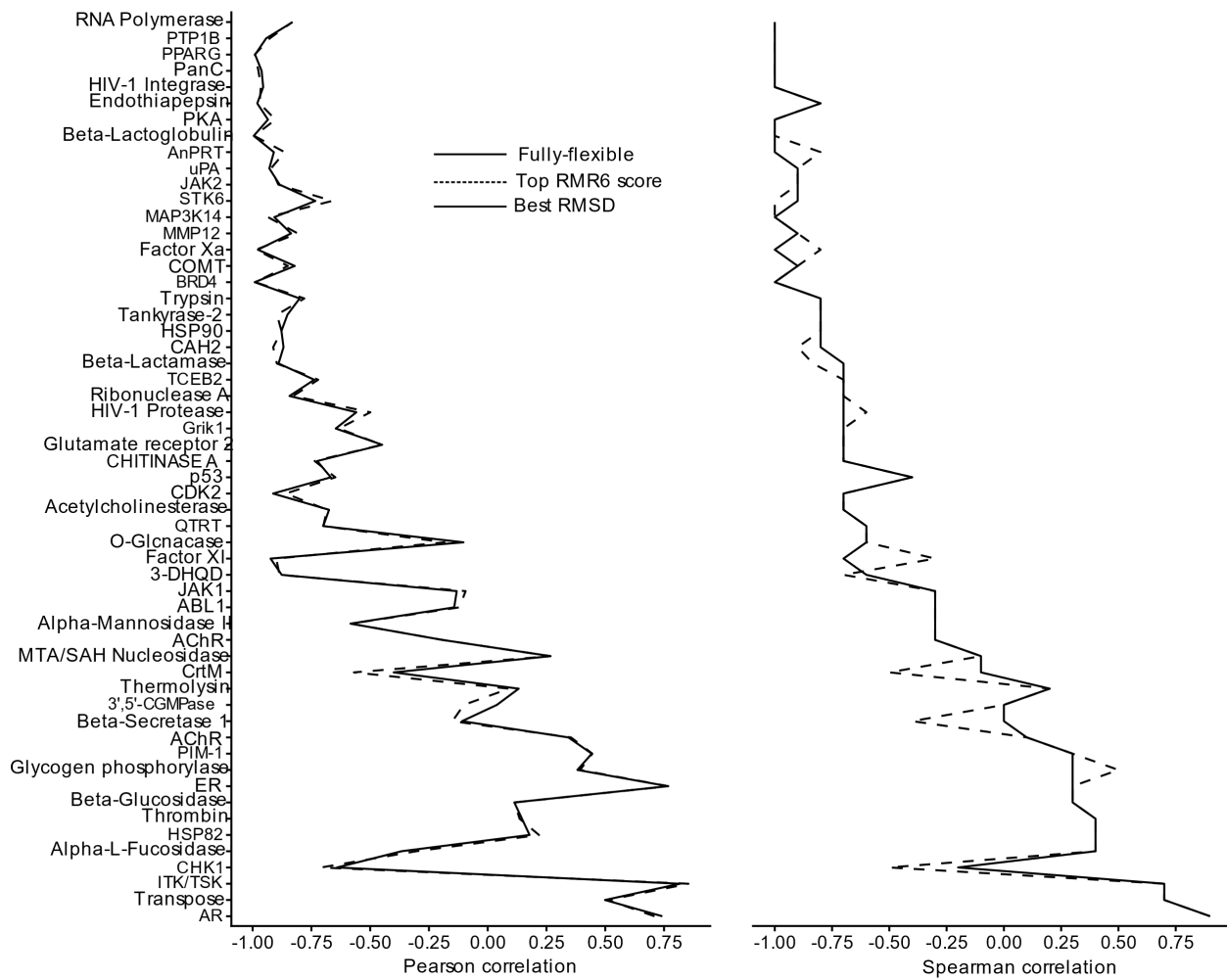


Figure S12: Fully flexible protein docking correlations between the RMC15 score and the measured pKd/pKi of the compounds in the PDBbind for each protein target. The representative docked ligand pose for ranking was selected with either the lowest RMSD or the best RMR6 score criterion.

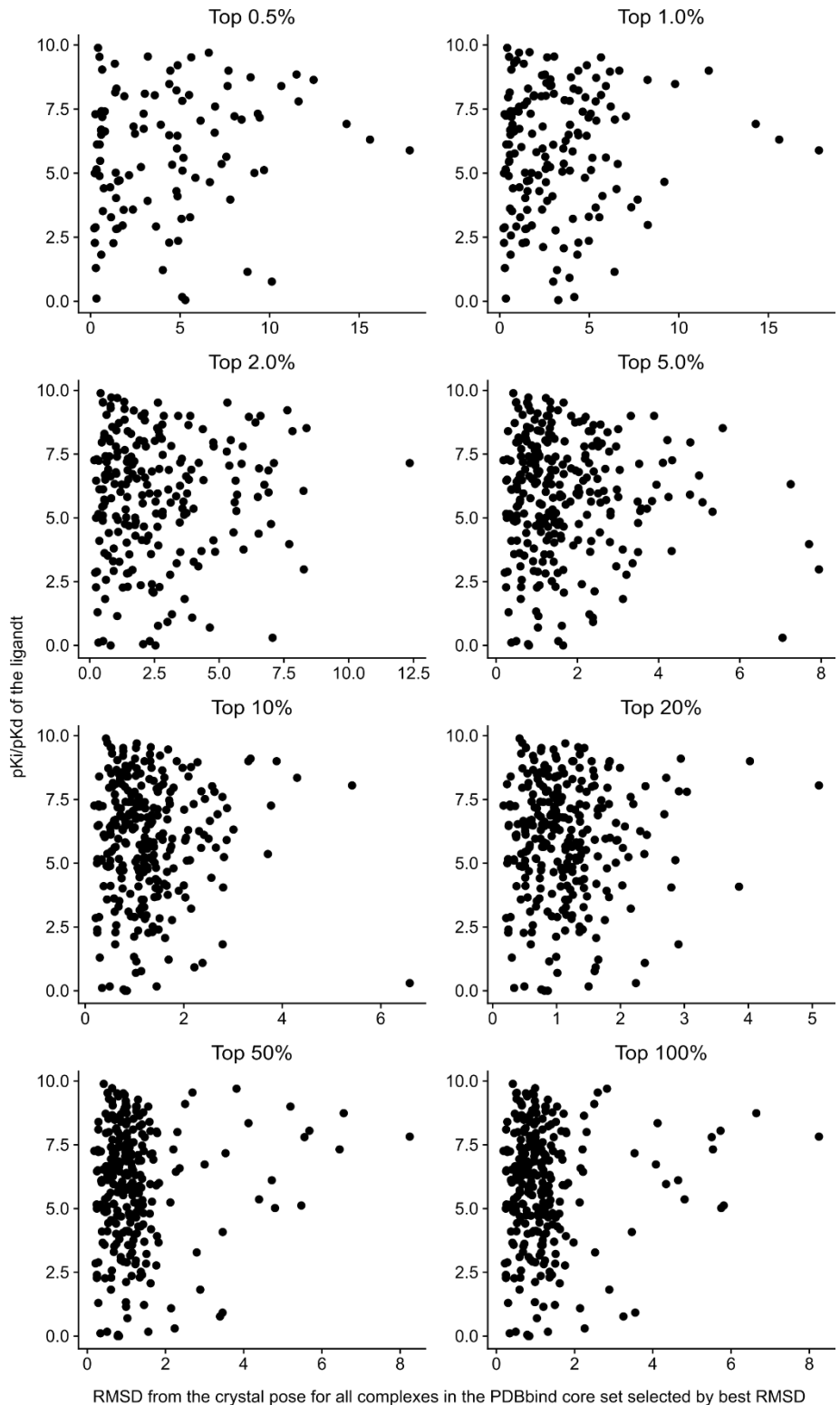


Figure S14: Plots of the ligand pKi/pKd against the best pose RMSD obtained using the semi-flexible method broken down by the ‘Top Percent’ parameter. These plots show there is no relationship between RMSD and pKi.

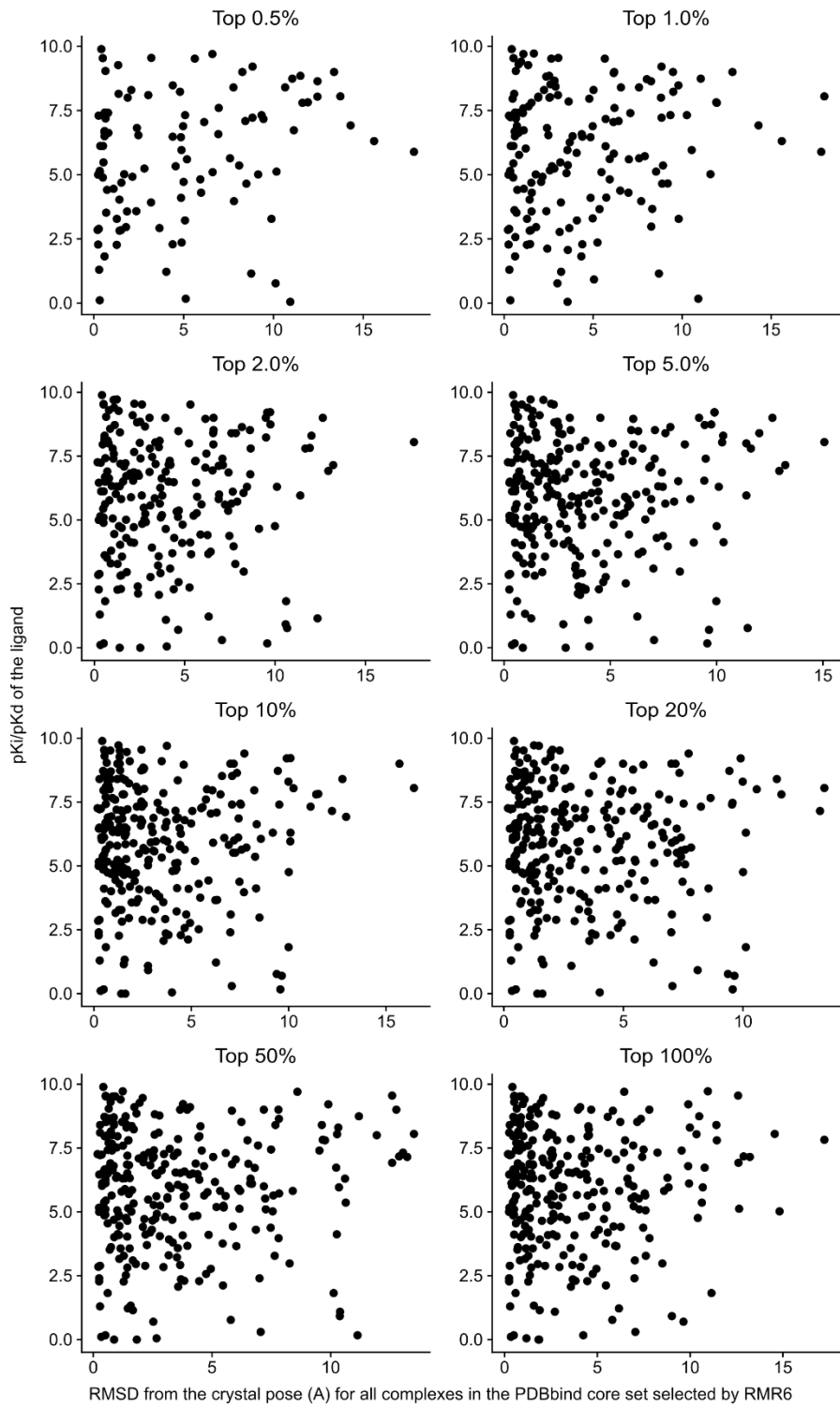


Figure S14: Plots of the ligand pK_i/pK_d against the RMR selected pose RMSD obtained using the semi-flexible method broken down by the 'Top Percent' parameter. These plots show there is no relationship between RMSD and pK_i when the pose is selected by RMR6..

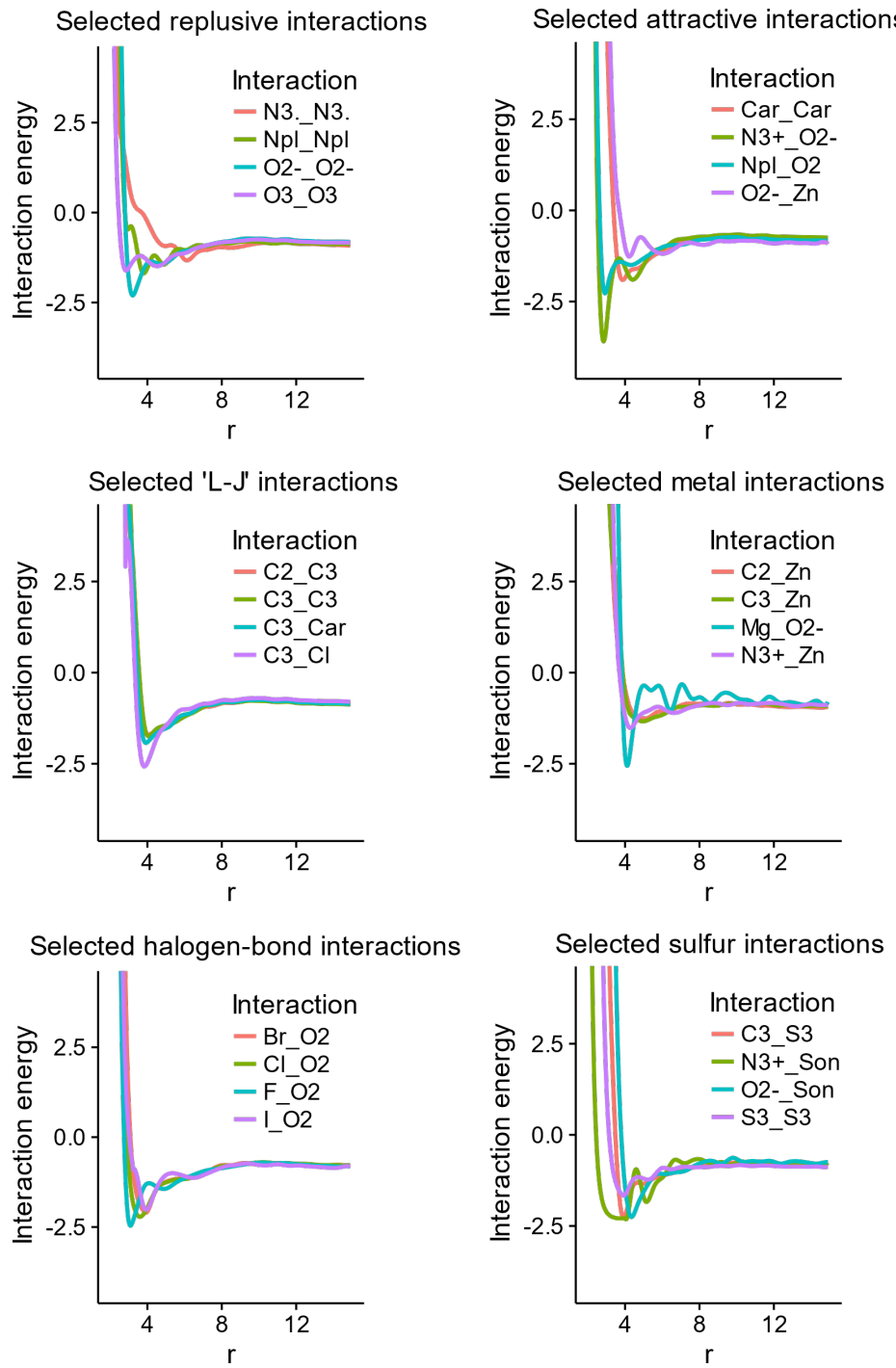


Figure S15: Interaction potentials for selected IDATM atom type pairs in the RMC15 objective function. These interactions are selected due to their conventionally repulsive/attractive/neutral nature, or due to their interest in drug discovery.